Main-Group Elements

DOI: 10.1002/ange.201311104

# Catalytic Transfer Hydrogenation by a Trivalent Phosphorus Compound: Phosphorus-Ligand Cooperation Pathway or $P^{III}/P^{V}$ Redox Pathway?**

*Guixiang Zeng, Satoshi Maeda, Tetsuya Taketsugu, and Shigeyoshi Sakaki**

***Abstract:*** *Main-group-element catalysts are a desirable alternative to transition-metal catalysts because of natural abundance and cost. However, the examples are very limited. Catalytic cycles involving a redox process and E-ligand cooperation (E = main-group element), which are often found in catalytic cycles of transition-metal catalysts, have not been reported. Herein theoretical investigations of a catalytic hydrogenation of azobenzene with ammonia–borane using a trivalent phosphorus compound, which was experimentally proposed to occur through $P^{III}/P^{V}$ redox processes via an unusual pentavalent dihydridophosphorane, were performed. DFT and ONIOM(CCSD(T):MP2) calculations disclosed that this catalytic reaction occurs through a P-O cooperation mechanism, which resembles the metal-ligand cooperation mechanism of transition-metal catalysts.*

Main-group-element compounds experienced a renaissance in the last decade because of their excellent reactivities, which are similar to those of transition-metal complexes.[1] For instance, carbene and acetylene analogues of compounds derived from heavy main-group elements are reactive for H–H σ-bond activation by oxidative addition,[1a,2] and the Ge–H bond is reactive for the insertion reactions of C≡C and C=O bonds.[1b,3] Though these are essentially the same as the elementary steps in the catalytic reactions by transition-metal complexes, full catalytic cycles by main-group-element compounds are limited,[1c] except for the catalysis of several frustrated Lewis pairs.[4] As is well-known, the catalytic cycles involving the metal-ligand cooperation and the redox process are often found in the chemistry of transition-metal complexes, but they have not been reported for main-group-element compounds. Recently, Radosevich and co-workers[5] reported an interesting catalytic reaction involving the trivalent phosphorus compound 10-P-3 ADPO **1P**,[6,7] and proposed a catalytic cycle proceeding by $P^{III}/P^{V}$ redox processes (Scheme 1). In this reaction, **1P** reacts with ammonia–borane to afford a pentavalent dihydridophosphorane, 10-P-5 ADPO·$(H)_2$ **4PP**, which catalyzes the hydrogenation of azobenzene to regenerate **1P**. However, the mechanistic details of these reactions and the role of **4PP** are still unclear. Such knowledge is necessary for further development of the chemistry of main-group-element compounds.

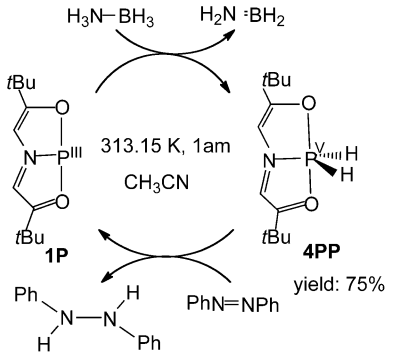


***Scheme 1.*** Catalytic cycle of transfer hydrogenation by **1P**.

In this work, we theoretically investigated all the reaction processes involved in Scheme 1. Geometry optimizations were carried out by the DFT[8] method using the B3PW91 functional,[9] and the AFIR method[10] was employed for optimizing several transition states. Electronic energies were calculated by the ONIOM(CCSD(T):MP2) method[11] in acetonitrile solution, where the CPCM model[12] was employed. Gaussian 09[13] was used herein (see the Supporting Information for computational details). Throughout this paper, the discussion is presented based on the Gibbs energy changes relative to the sum of the energies of the reactants (**1P** + ammonia–borane + azobenzene), unless otherwise noted. For convenience, the tri-ligated moiety coordinating with the phosphorus center in **1P** is hereafter referred to as an ONO ligand.

For the dehydrogenation reaction of ammonia–borane, three kinds of reaction pathways are considered to be possible. One is the concerted oxidative addition, which occurs only on the phosphorus center via the transition-state $\mathbf{TS_{1P/4PP}}$ to directly afford **4PP** (Figure 1). This pathway requires a large Gibbs activation energy ($\Delta G^{0\ddagger}$) of 42.7 kcal $mol^{-1}$, thus indicating that this reaction pathway is difficult (Figure 2).

The second is the stepwise pathway, which occurs through the oxidative addition of the B–H or N–H σ bond to the

[*] Dr. G. Zeng, Prof. Dr. S. Sakaki
Fukui Institute for Fundamental Chemistry, Kyoto University
Takano-Nishihiraki-cho 34-4, Sakyo-ku, Kyoto 606-8103 (Japan)
E-mail: sakaki.shigeyoshi.47e@st.kyoto-u.ac.jp
Prof. Dr. S. Maeda, Prof. Dr. T. Taketsugu
Department of Chemistry, Faculty of Science, Hokkaido University
North-10, west-8, Kita-ku, Sapporo 060-0810 (Japan)

[**] This work was supported by the Grants-in-Aid from Ministry of Education, Culture, Science, Sport, and Technology through Grants-in-Aid of Specially Promoted Science and Technology (No. 22000009). We are also grateful to the computational facility at the Institute of Molecular Science, Okazaki (Japan).

Supporting information for this article is available on the WWW under http://dx.doi.org/10.1002/anie.201311104.

  

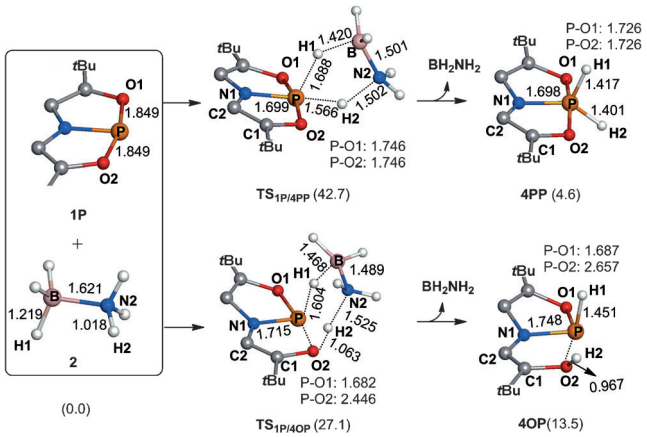


***Figure 1.*** Geometry changes in the concerted oxidative addition and the P-O cooperation reaction pathways. Distances are in Å. The Gibbs energy changes are given within parentheses (kcal mol$^{-1}$).

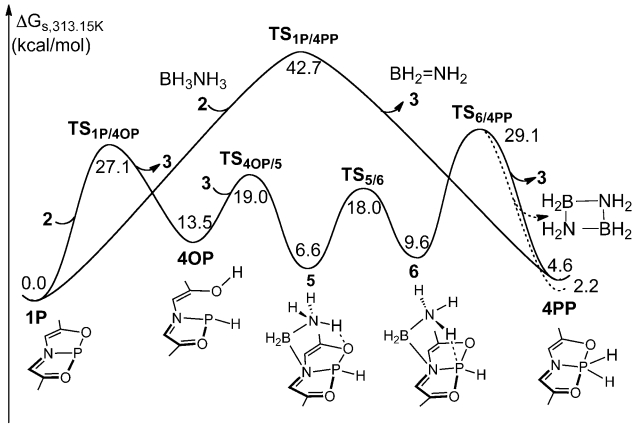


***Figure 2.*** The Gibbs energy changes (in kcal mol$^{-1}$) for the dehydrogenation reaction of ammonia–borane by **1P**.

phosphorus center followed by a β-hydrogen abstraction (see Figure S2 in the Supporting Information). However, the Gibbs activation energy of the oxidative additions of the B–H and N–H σ-bonds are too large (70.0 and 60.4 kcal mol$^{-1}$, respectively) for the reaction to occur. This energy is in contrast to the facile oxidative addition of the B–H σ-bond of ammonia–borane to the iridium(I) complex.[14]

The third is the P-ONO cooperation pathway, in which the phosphorus center and one atom of the ONO ligand cooperatively react with ammonia–borane (Figure 1). The P-O cooperation pathway is the most favorable with a moderate $\Delta G^{0\ddagger}$ value of 27.1 kcal mol$^{-1}$, which is much smaller than those of the aforementioned pathways. In this step, the intermediate **4OP** is formed via the transition-state **TS$_{1P/4OP}$** with the release of $NH_2$=$BH_2$. In **4OP**, the phosphorus center has a usual three-coordinate structure, where the P–O2 bond is broken (2.657 Å). This P-O cooperative reaction is similar to the dehydrogenation of alcohols by transition-metal complexes with pincer ligands.[15] In contrast, the P-C1, P-C2, and P-N1 cooperation pathways require much larger $\Delta G^{0\ddagger}$ values (56.1, 35.8, and 41.1 kcal mol$^{-1}$, respectively; see Figure S3 in the Supporting Information). It should be noted that the phosphorus-ligand cooperation mechanism found here is the first of this type for main-group-element compounds.

As shown in Figure 2, **4OP** is less stable than **4PP** by 8.9 kcal mol$^{-1}$. Also, **4PP** was experimentally isolated. Hence, we investigated the isomerization of **4OP** into **4PP**. In a one-step intramolecular pathway, the H2 atom directly migrates from the O2 atom to the phosphorus center to yield **4PP**. However, this isomerization needs a large $\Delta G^{0\ddagger}$ value of 42.2 kcal mol$^{-1}$ (see Figure S4 in the Supporting Information). Several stepwise intramolecular pathways, in which the H2 atom transfers from the O2 atom to the phosphorus center via the C1, C2, or N1 atoms, also require large $\Delta G^{0\ddagger}$ values (see Figure S4).

Then, we investigated the $NH_2$=$BH_2$-assisted transformation of **4OP** into **4PP**, considering that one $NH_2$=$BH_2$ molecule was produced by the dehydrogenation reaction of ammonia–borane. As shown in Figure 3, the $BH_2$ moiety of $NH_2$=$BH_2$ interacts with the N1 atom of **4OP** because the $BH_2$ moiety is a Lewis acid and the N1 moiety is a Lewis base. Simultaneously, the N2 atom of $NH_2$=$BH_2$ lifts the H2 atom from the O2 atom. This step occurs through the transition state **TS$_{4OP/5}$** to form the more stable intermediate **5**. In **5**, the $NH_2$ group is converted into an $NH_3$ group and a B–N1 covalent bond is formed. At the same time, the B=N2 bond changes into a B–N2 bond (see Figure 3 for bond distances). Interestingly, the P–N1 bond is kept and the phosphorus center has a four-coordinate structure. After that, the $BH_2$-$NH_3$ moiety rotates around the B–N1 bond to bring the H2 atom toward the phosphorus atom via the transition state **TS$_{5/6}$** to afford the intermediate **6**. In **6**, the P–N1 bond is broken and the phosphorus center returns to a usual $sp^3$-like structure with three-coordinate bonds. Finally, the H2 atom moves to the phosphorus atom via the transition state **TS$_{6/4PP}$** to afford **4PP**. In this process, the P–N1 bond is formed again and the phosphorus center changes from the three-coordinate structure to a five-coordinate hypervalent structure. Along with these structural changes, the oxidation state of the phosphorus atom changes from +III to +V. The last step is the rate-determining step with a $\Delta G^{0\ddagger}$ value of 29.1 kcal mol$^{-1}$, which is much smaller than those of the intramolecular isomerizations.

Next, an intermolecular hydrogen exchange pathway was also examined, which involves mutual hydrogen transfers between two **4OP** molecules via **TS$_{4OP/4PP}$** (Figure 3). **TS$_{4OP/4PP}$** is not symmetrical as the O2-H2 (1.025 Å) and O2′-H2′ (1.457 Å) distances are very different. As shown in Figure 2, **4PP** is somewhat less stable than the reactants (**1P** + ammonia–borane) by 4.6 kcal mol$^{-1}$. When the cyclic dimerization of $NH_2$=$BH_2$ to $(NH_2BH_2)_2$ is considered, the endothermicity decreases but the reaction is still endothermic by 2.2 kcal mol$^{-1}$ (see the dashed line in Figure 2). These results are consistent with the experimental observation that **4PP** is converted into **1P** with the release of $H_2$.[17]

In summarizing the above results, **1P** reacts with ammonia–borane through the P-O cooperation pathway to afford the intermediate **4OP**. Then, **4OP** isomerizes into **4PP** either with the assistance of $NH_2$=$BH_2$ or through an intermolecular hydrogen transfer between two **4OP** molecules.[18]

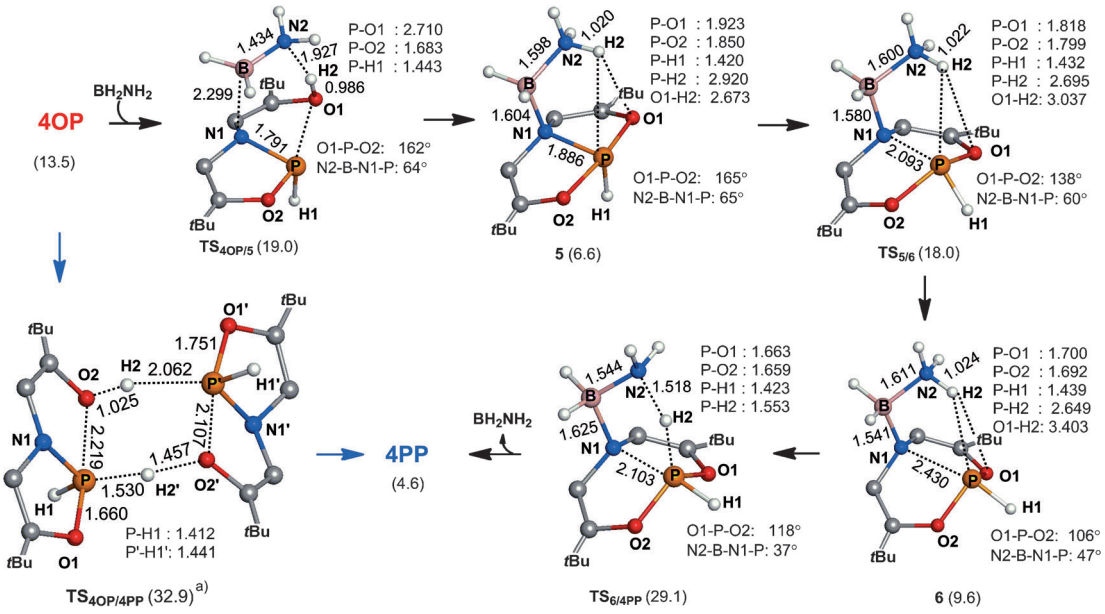


***Figure 3.*** Geometry changes in the isomerization of **4OP** into **4PP**; distances are in Å. B3PW91-calculated energy values. The Gibbs activation energy is comparable with that of the $NH_2$=$BH_2$-assisted pathway.[16]

**4PP** was experimentally proposed to be an active species in the hydrogenation reaction of **7** with ammonia–borane. Considering this proposal, we investigated the reaction of **4PP** with **7**. When **7** approaches **4PP**, the H2 atom migrates from the phosphorus atom to the N3 atom via the transition-state $\mathbf{TS_{4PP/8}}$ to form the intermediate **8** (Figure 4). The $\Delta G^{0\ddagger}$ and $\Delta G^{0}$ values are 27.5 and 29.4 kcal mol$^{-1}$, respectively.[19] The intermediate **8** is understood to be an ion-pair between a phosphonium cation and a deprotonated diphenylhydrazine anion [PhN-NHPh]$^-$. Then, the N4 atom of the [PhN-NHPh]$^-$ is bound to the cationic phosphorus center to form a very stable intermediate (**9**) through a rotation of the [PhN-NHPh]$^-$ moiety. Though the transition state could not be optimized, it is likely that this process easily occurs because the [PhN-NHPh]$^-$ moiety is sufficiently distant from the phosphorus center. This step is significantly exothermic by 39.8 kcal mol$^{-1}$. At last, the reductive elimination occurs to yield diphenylhydrazine (**10**) and regenerate **1P** with a large $\Delta G^{0\ddagger}$ value of 43.2 kcal mol$^{-1}$ relative to **9** which is the most stable intermediate.

Considering that the insertion of the C=O double bond of a ketone into the Ge–H bond was experimentally and theoretically reported,[1b,3,20] we investigated the insertion reaction of the N=N double bond of **7** into a P–H bond. However, it requires a large $\Delta G^{0\ddagger}$ value (53.5 kcal mol$^{-1}$; see Figure S5 in the Supporting Information). All these results indicate that **4PP** is not an active species for the hydrogenation of **7**.

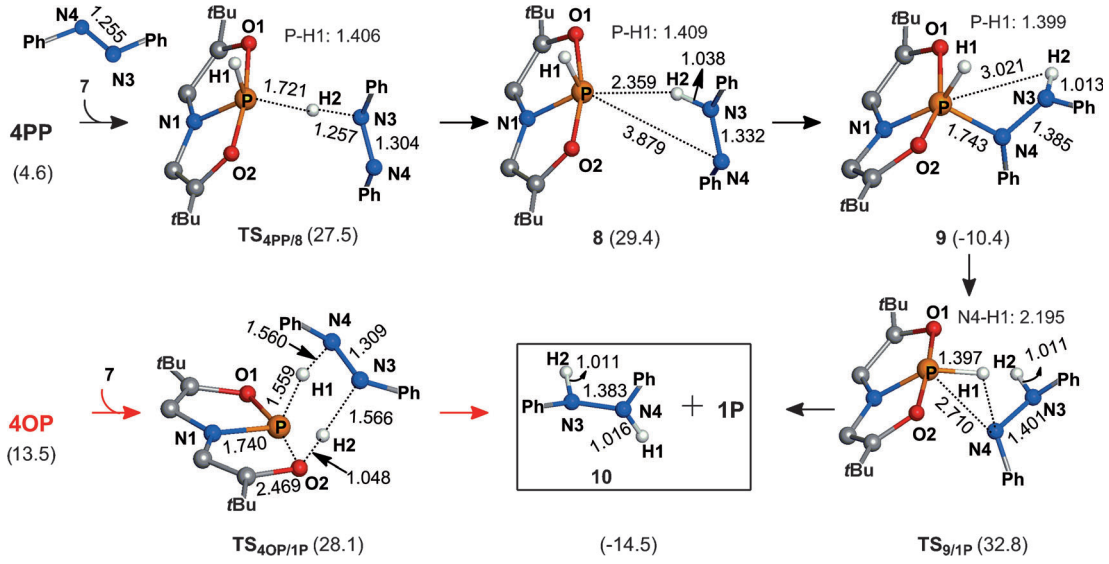


***Figure 4.*** Geometry changes in the hydrogenation reaction of **7** by **4PP** and **4OP**; distances are in Å.

Besides **4PP**, **4OP** is expected to be able to perform the hydrogenation of **7**, because the H1 and H2 atoms of **4OP** are considered to be reactive for the hydrogenation reaction. This reaction occurs through a concerted transition state ($\mathbf{TS_{4OP/1P}}$) to produce **1P** and **10** (Figure 4). The $\Delta G^{0\neq}$ value is 28.1 kcal mol$^{-1}$, which is much smaller than that of the hydrogantion reaction by **4PP** discussed above. This $\Delta G^{0\neq}$ value is not very different from the experimental value (23.7 kcal mol$^{-1}$ at 313.15 K), where the experimental $\Delta H^{0\neq}$ and $\Delta S^{0\neq}$ values [$(12.4 \pm 0.7)$ kcal mol$^{-1}$ and $(-36 \pm 7)$ eu, respectively][5] were employed. Based on these results, it should be concluded that not **4PP** but **4OP** is the active species for the transfer hydrogenation reaction.

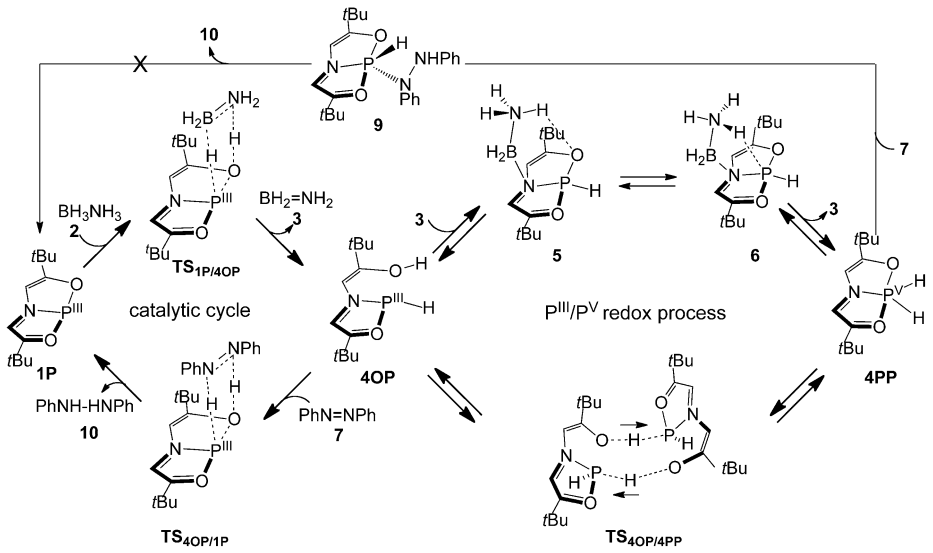


***Scheme 2.*** Catalytic cycle of transfer hydrogenation by **1P** by the P-O cooperation and mutual transformation between **4OP** and **4PP** by the $P^{III}/P^{V}$ redox processes.

Radosevich et al. reported that **4PP** could catalyze the transfer hydrogenation but less effeciently than **1P**.[5] This fact is explained, as follows: **4PP** is transformed into **4OP** by the $NH_2$=$BH_2$-assisted or the intermolecular hydrogen transfer pathway (Figure 3). Then, **4OP** reacts with **7** to regerenate **1P** with the release of **10**. After that, the catalytic hydrogenation is performed by **1P**. Besides the transformation to **4OP**, **4PP** can also react with **7**. This reaction leads to the very stable intermediate **9** as discussed above. Note that it is difficult for **9** to undergo both β-hydrogen abstraction and the reductive elimination (Figure 4). This feature means that some amount of **4PP** is trapped as **9** during the reaction. As a result, the catalytic hydrogenation by **4PP** occurs more slowly than that by **1P**.

We investigated the substituent effect on the activity of the catalyst. The substitution of $CF_3$ for *t*Bu somewhat decreases the $\Delta G^{0\neq}$ values for $\mathbf{TS_{1P/4OP}}$ and $\mathbf{TS_{4OP/1P}}$ to 20.9 kcal mol$^{-1}$ and 23.5 kcal mol$^{-1}$, respectively, thus indicating that the electron-withdrawing group is favorable for the catalytic reaction (see Figure S6 in the Supporting Information). In contrast, the substitution of H for *t*Bu changes the $\Delta G^{0\neq}$ value for $\mathbf{TS_{1P/4OP}}$ very little and moderately decreases the $\Delta G^{0\neq}$ value for $\mathbf{TS_{4OP/1P}}$, thus indicating that the bulk of the substituent is not important (see Figure S7 in the Supporting Information). Also, the transformation of **4OP** into **4PP** is little influenced by both substitutions (see Figure S8 in the Supporting Information).

In conclusion, the mechanistic details of the transfer hydrogenation reaction by a trivalent phosphorus compound **1P** were theoretically disclosed here. As summarized in Scheme 2: 1) the catalytic cycle occurs through a new concerted P-O cooperation mechanism, 2) the active species of the transfer hydrogenation is **4OP**, which is produced from **1P** through the dehydrogenation of ammonia–borane, 3) this P-O cooperative reaction resembles the metal-ligand cooperation reaction by the transition-metal complex with a pincer ligand, 4) the $P^{III}/P^{V}$ redox reaction certainly occurs in the mutual conversions between **4OP** and **4PP**, but it is not involved in the catalytic cycle, and 5) the substitution of the electron-withdrawing $CF_3$ group for *t*Bu improves the catalytic activity of the trivalent phosphorus compound.

Received: December 21, 2013
Published online: March 25, 2014

**Keywords:** density functional calculations · hydrogenation · main-group elements · phosphorus · redox chemistry

[1] a) P. P. Power, *Nature* **2010**, *463*, 171 – 177; b) S. Mandal, H. W. Roesky, *Acc. Chem. Res.* **2012**, *45*, 298 – 307; c) A. Schulz, A. Villinger, *Angew. Chem.* **2012**, *124*, 4602 – 4604; *Angew. Chem. Int. Ed.* **2012**, *51*, 4526 – 4528.

[2] a) G. H. Spikes, J. C. Fettinger, P. P. Power, *J. Am. Chem. Soc.* **2005**, *127*, 12232 – 12233; b) Z. Zhu, X. Wang, Y. Peng, H. Lei, J. C. Fettinger, E. Rivard, P. P. Power, *Angew. Chem.* **2009**, *121*, 2065 – 2068; *Angew. Chem. Int. Ed.* **2009**, *48*, 2031 – 2034.

[3] a) A. Jana, D. Ghoshal, H. W. Roesky, I. Objartei, G. Schwab, D. A. Stalke, *J. Am. Chem. Soc.* **2009**, *131*, 1288 – 1293; b) A. Jana, H. W. Roesky, C. Shulzke, A. Döring, *Angew. Chem.* **2009**, *121*, 1126 – 1129; *Angew. Chem. Int. Ed.* **2009**, *48*, 1106 – 1109.

[4] a) E. M. Leitao, T. Jurca, I. Manners, *Nat. Chem.* **2013**, *5*, 817 – 829; b) J. D. Protasiewicz, *Eur. J. Inorg. Chem.* **2012**, 4539 – 4549; c) D. W. Stephan, *Comprehensive Inorganic Chemistry II* (Eds.: J. Reedijk, K. Poeppelmeier), Elsevier, Oxford, **2013**; d) D. W. Stephan, *Topics in Current Chem.: Frustrated Lewis Pairs I* (Ed.: D. W. Stephan, G. Erker), Springer, Berlin, **2013**, pp. 1 – 44.

[5] N. L. Dunn, M. Ha, A. T. Radosevich, *J. Am. Chem. Soc.* **2012**, *134*, 11330 – 11333.

[6] a) S. A. Culley, A. J. Arduengo, *J. Am. Chem. Soc.* **1984**, *106*, 1164 – 1165; b) A. J. Arduengo, C. A. Stewart, F. Davidson, D. A. Dixon, J. Y. Becker, S. A. Culley, M. B. Mizen, *J. Am. Chem. Soc.* **1987**, *109*, 627 – 647.

[7] E. E. Coyle, C. J. O'Brien, *Nat. Chem.* **2012**, *4*, 779 – 780.

[8] a) P. Hohenberg, W. Kohn, *Phys. Rev.* **1964**, *136*, B864 – B871; b) W. Kohn, L. J. Sham, *Phys. Rev.* **1965**, *140*, A1133 – A1138.

[9] a) A. D. Becke, *Phys. Rev. A* **1988**, *38*, 3098 – 3100; b) A. D. Becke, *J. Chem. Phys.* **1993**, *98*, 5648 – 5652; c) J. P. Perdew in *Electronic Structure of Solids*, 91th ed. (Eds.: P. Ziesche, H. Eschrig), Akademie Verlag, Berlin, **1991**; d) K. Burke, J. P. Perdew, Y. Wang in *Electronic Density Functional Theory: Recent Progress and New Directions* (Eds.: J. F. Dobson, G. Vignale, M. P. Das), Plenum, New York, **1998**.

[10] a) S. Maeda, K. Morokuma, *J. Chem. Theory Comput.* **2011**, *7*, 2335 – 2345; b) S. Maeda, K. Ohno, K. Morokuma, *Phys. Chem. Chem. Phys.* **2013**, *15*, 3683 – 3701; c) S. Maeda, T. Taketsugu, K. Morokuma, *J. Comput. Chem.* **2014**, *35*, 166 – 173.

[11] S. Dapprich, I. Komáromi, K. S. Byun, K. Morokuma, M. J. Frisch, *J. Mol. Struct. (Theochem)* **1999**, *462*, 1 – 21.

[12] J. Tomasi, B. Mennucci, R. Cammi, *Chem. Rev.* **2005**, *105*, 2999 – 3093.

[13] M. J. Frisch, et al. *Gaussian 09*, revision B.01; Gaussian, Inc.: Wallingford, CT, **2009**.

[14] A. Rossin, M. Caporali, L. Gonsalvi, A. Guerri, A. Lledós, M. Peruzzini, F. Zanobini, *Eur. J. Inorg. Chem.* **2009**, 3055 – 3059.

[15] a) C. Gunanathan, D. Milstein, *Acc. Chem. Res.* **2011**, *44*, 588 – 602; b) G. Zeng, Y. Guo, S. Li, *Inorg. Chem.* **2009**, *48*, 10257 – 10263; c) G. Zeng, S. Li, *Inorg. Chem.* **2011**, *50*, 10572 – 10580; d) H. Li, X. Wang, F. Huang, G. Lu, J. Jiang, Z. Wang, *Organometallics* **2011**, *30*, 5233 – 5247.

[16] The B3PW91-calculated $\Delta G^{0\ddagger}$ values are 32.1 and 32.9 kcal mol$^{-1}$ for $\mathbf{TS_{6/4PP}}$ and $\mathbf{TS_{4OP/4PP}}$, respectively. Only here, the B3PW91-calculated value is presented because the ONIOM-(CCSD(T):MP2) calculation is difficult to be carried out because of the large size of $\mathbf{TS_{4OP/4PP}}$.

[17] A. J. Arduengo III, H. V. R. Dias, J. C. Calabrese, *Phosphorus Sulfur Relat. Elem.* **1987**, *30*, 341 – 350.

[18] In the early stage of the reaction, the $BH_2=NH_2$-assisted isomerization mainly occurs, while the intermolecular hydrogen exchange would occur when the concentration of **4OP** becomes larger.

[19] This unreasonable energy change may arise from the difference in the quality between the ONIOM and DFT methods. In DFT calculation, **8** is lower than $\mathbf{TS_{4PP/8}}$ by 2.2 kcal mol$^{-1}$ in Gibbs energy.

[20] N. Takagi, S. Sakaki, *J. Am. Chem. Soc.* **2013**, *135*, 8955 – 8965.

  